BJPS

Brazilian Journal of
Pharmaceutical Sciences

http://dx.doi.org/10.1590/s2175-97902023e22304

Article

Effects of Chitosan Nanoparticles with Long Synthetic siRNAs Targeting VEGF in Triple-Negative Breast Cancer Cells

Birnur Cömez[1*], Jülide Akbuğa[2]

[1]Department of Pharmaceutical Biotechnology, Faculty of Pharmacy, Marmara University, Istanbul, Turkey, [2]Department of Pharmaceutical Technology, Faculty of Pharmacy, Istanbul Medipol University, Istanbul, Turkey

Vascular endothelial growth factor (VEGF) is an essential angiogenic factor in breast cancer development and metastasis. Small interfering RNAs (siRNAs) can specifically silence genes via the RNA interference pathway, therefore were investigated as cancer therapeutics. In this study, we investigated the effects of siRNAs longer than 30 base pairs (bp) loaded into chitosan nanoparticles in triple-negative breast cancer cells, compared with conventional siRNAs. 35 bp long synthetic siRNAs inhibited VEGF gene expression by 51.2% and increased apoptosis level by 1.75-fold in MDA-MB-231 cell lines. Furthermore, blank and siRNA-loaded chitosan nanoparticles induced expression of IFN-γ in breast cancer cells. These results suggest that long synthetic siRNAs can be as effective as conventional siRNAs, when introduced into cells with chitosan nanoparticles.

Keywords: siRNA. VEGF. Chitosan. Nanoparticle. Breast cancer.

INTRODUCTION

RNA interference (RNAi) is a potent gene silencing method triggered by double-stranded RNAs (dsRNAs). The effectors of RNAi are small interfering RNAs (siRNAs) that are produced from longer dsRNA precursors by Dicer, which is an RNAse III endonuclease. siRNAs are commonly between 21-23 bp in length with 2-base 3'-overhangs and have sequence-specific gene silencing capability. siRNAs are recognized by the RNA-induced silencing complex (RISC) and the antisense strand of siRNA serves as a guide for degradation of target mRNA (Kim, Rossi, 2008; Ozcan *et al*., 2015). Although siRNAs have the potential to specifically inhibit the expression of any gene, many challenges including rapid degradation by nucleases in biological fluids and the delivery of siRNA to target cells and tissues, limit the clinical use of RNAi systems. Therefore, the development of appropriate carrier systems is very important for siRNA delivery (Leung *et al*., 2014).

In vivo, double-stranded RNAs (dsRNAs) that are longer than 23-nucleotides (nt), are cleaved by Dicer into short siRNA products (Amarzguioui *et al*., 2006). Studies of the effects of different 5' and 3' end structures of dsRNAs, showed that slightly longer siRNAs have higher activity than synthetic 21-bp siRNA targeting the same region (Kim *et al*., 2005). The use of dsRNAs longer than 30 bp in mammalian systems was initially thought to be unsafe due to activation of interferons and the induction of gene inhibition, independent of the dsRNA sequence (Dahlgren, Wahlestedt, Thonberg 2006; Elbashir *et al*., 2001). However, it has been reported that multi-targeted long synthetic siRNAs (38 bp) simultaneously suppressed the expression of two genes without triggering interferon response. Synthetic dsRNAs of 34 and 38 bp length specifically inhibited the target gene without an antiviral response (Chang *et al*., 2009).

Breast cancer is the most common malignancy and the second commonest cause of tumour-related death among women in the world. Mortality rates have

***Correspondence:** B. Cömez. Department of Pharmaceutical Biotechnology. Faculty of Pharmacy. Marmara University. Başıbüyük Yolu, 34854 4/A. Maltepe, Istanbul, Turkey. Phone: +90 507 828 35 90. E-mail: birnur.comez@marmara.edu.tr. ORCID: 0000-0002-9961-5560

decreased in recent years because of early diagnosis and advanced treatment methods. Metastasis is the main cause of death from breast cancer. Non-metastatic breast cancer is considered curable as the five-year overall survival is greater than 80%, whereas in metastatic disease there is only a 25% reduction in the five-year overall survival rate (Zarychta, Ruszkowska-Ciastek, 2022).

Angiogenesis plays an important role in cancer growth and metastasis, as it provides the formation of blood vessels that will supply oxygen and nutrients to cancer cells. VEGF is one of the major regulators of vascular growth and angiogenesis. Altered expression levels of VEGF is shown to have significant effects on tumour growth, response to therapy, and survival in breast cancer, which makes VEGF a promising therapeutic target (Ayoub *et al*, 2022). Both monotherapy and combination therapy applications of siRNA targeting VEGF were shown to inhibit tumour growth and angiogenesis (Chen *et al*., 2017; Dong *et al*., 2015; Feng *et al*., 2014).

Chitosan and its derivatives have been extensively investigated for siRNA delivery due to these polysaccharides being biodegradable, biocompatible, and non-toxic. Chitosan is a cationic polysaccharide with positively charged amines that interact electrostatically with negatively charged nucleic acids to form nano-sized structures (Rudzinski, Aminabhavi, 2010).

This study aimed to investigate the effects of chitosan nanoparticles as a carrier of siRNAs longer than 30 bp and to compare with conventional siRNA in breast cancer cells. For this purpose, we determined VEGF expression, apoptosis, and interferon-gamma (IFN-γ) protein levels after delivery of VEGF-targeted siRNA via chitosan nanoparticles into MDA-MB-231 cell lines.

MATERIAL AND METHODS

Material

A core sequence consisting of 19-nt was selected against VEGF-A mRNA (Accession No. NM_001025366.2) using BLOCK-iT RNAi Designer (Invitrogen, CA, USA) to design siRNAs. The core sequence was extended to the 3' end of the target gene such that it contains 33-nt. The sequences of 21-bp VEGF-A siRNA were 5'-GCAGCUACUGCCAUCCAAUdTdT-3' (sense) and 5'-AUUGGAUGGCAGUAGCUGCdTdT -3' (antisense). The sequences of 35-bp VEGF-A siRNA were 5'-GCAGCUACUGCCAUCCAAUCGAGACCCUGGUGGdTdT-3'(sense) and 5'-CCACCAGGGUCUCGAUUGGAUGGCAGUAGCUGCdTdT-3' (antisense). 5′-FLO siRNA was labelled with fluorescein and used to monitor cellular uptake. All siRNA sequences were analysed by BLAST to verify the absence of significant homology with other human genes. All siRNAs were synthesised by Invitrogen (Carlsbad, CA, USA).

Low molecular weight chitosan (70 kDa, 75–85% degree of deacetylation) and pentasodium tripolyphosphate (TPP) were obtained from Sigma-Aldrich (St. Louis, MO, USA). DMEM, fetal bovine serum (PAN Biotech, Aidenbach, Germany) was used in the cell culture studies. VEGF and IFN-γ ELISA kits were purchased from Invitrogen (Carlsbad, CA, USA). ApoTarget™ Caspase-3 protease assay kit was obtained from Life Technologies (Carlsbad, CA, USA). Other chemicals and reagents were of the analytical and molecular grade.

Cell culture

Transfection studies were performed in MDA-MB-231 breast cancer cell lines (ATCC, Manassas, VA, USA). According to immunohistochemical analysis, MDA-MB-231 is ER-negative, PR-negative, and HER2-negative (Holliday, Speirs, 2011). The cells were cultured in DMEM supplemented with 10% fetal bovine serum, 100 U mL^{-1} penicillin, and 100 μg mL^{-1} streptomycin (PAN Biotech, Aidenbach, Germany). All cell lines were incubated at 37°C and 5% CO_2 (Sanyo MCO-20AIC CO_2 Incubator, Japan).

Preparation of siRNA-loaded chitosan nanoparticles

Chitosan nanoparticles containing siRNA were prepared by ionic gelation using TPP as the polyanionic agent (Calvo *et al*., 1997). 60 μg of siRNA was added to 0.25% (w/v) TPP solution. This mixture was dropped into 0.25% (w/v) chitosan solution in 2% glacial acetic acid while stirring with a magnetic stirrer. After the dropping process ended, it was stirred for 30 minutes at room temperature. The nanoparticles that formed were washed

with double distilled water three times and separated by centrifugation at 12.000 x g, then lyophilised (Leybold-Lyovac, Germany).

Characterisation of nanoparticles

The encapsulation efficiency of the siRNAs was determined by measuring the supernatants collected after centrifugation (12.000 x g, 15 min) at 260 nm with a UV-vis spectrophotometer (Shimadzu Biospec 1601, Shimadzu Scientific Instruments, Japan). siRNA concentrations were calculated from the supernatants using the standard curves of 21-bp and 35-bp siRNAs. The encapsulation efficiency of both siRNAs was calculated by the equation (Katas, Alpar, 2006):

$$\frac{\text{Concentration of siRNA added - Concentration of siRNA in supernatant}}{\text{Concentration of siRNA added}} \times 100$$

Morphological characterisation of siRNA-loaded chitosan nanoparticles was performed visually by transmission electron microscopy (TEM, JEM 1011; Jeol, Tokyo, Japan). The size and zeta potential of nanoparticles were measured by the Zetasizer Nano ZS (Malvern Instruments, UK). The samples were dispersed in double distilled water, and each measurement was performed in triplicate and at 25°C.

Gel retardation assay

The binding of siRNAs to chitosan nanoparticles was determined by 2% w/v agarose gel electrophoresis. 20 µl of siRNA-loaded chitosan nanoparticle suspension was loaded into agarose gel with a 5:1 dilution of loading dye. Electrophoresis was performed at 80mA for 30 minutes. Free siRNA was used as a control and siRNA bands were visualised by a UV transilluminator (Vilber Lourmat, France).

Serum stability of the nanoparticles

siRNA-loaded chitosan nanoparticles were suspended in 100 µl PBS (pH 7.4) buffer with 10% fetal bovine serum and incubated at 37°C. During the incubation, aliquots were taken at determined time intervals (0, 1, 4, 6, 24, and 48 h) and stored at -20°C until agarose gel electrophoresis analysis. The samples were incubated in a water bath at 80°C for 5 minutes. 1 µl heparin (5000 IU/ml) was added to each aliquot to displace the siRNA from the chitosan nanoparticles. The integrity of the siRNA was analysed by 2% agarose gel electrophoresis. Electrophoresis was carried out at a constant voltage of 200V for 30 min in 0.5x TBE buffer. siRNA bands were viewed under a UV transilluminator.

In vitro release study

Nanoparticles containing 10 µg siRNA were suspended in 1 ml of RNAse-free PBS (pH 7.4) and incubated in a shaking water bath at 37 °C. The samples were centrifuged at 14.000 x g for 30 min at different time intervals. The supernatants were removed for analysis and replaced with an equivalent volume of fresh PBS. The concentration of siRNA released in the supernatant was measured by a UV-vis spectrophotometer (Shimadzu UV1800, Shimadzu Scientific Instruments, Japan) at 260 nm (Raja, Katas, Wen, 2015). Each sample was studied in triplicate.

The release profiles of each nanoparticle were determined by plotting the percentage of cumulative siRNA release at different times. The release profiles of both nanoparticles were compared with the difference factor (f_1) and the similarity factor (f_2) by equations (1) and (2) (Cano-Vega, Deng, Pinal, 2021):

(1) $$f_1 = \{ \sum_{t=1}^{n} |R_t - T_t| / \sum_{t=1}^{n} R_t \} \times 100$$

(2) $$f_2 = 50 \times \log\{[1 + (1/n) \sum_{t=1}^{n} (R_t - T_t)^2]^{-0.5}\} \times 100$$

(n = number of timepoints; R_t = the released value of the reference at time t; T_t = the released value of the test at time t)

A model-dependent approach was used to determine the release kinetics of nanoparticles. The release data was applied to the mathematical equations of zero-order, first-order, Higuchi, Hixon-Crowell, and Korsmeyer-Peppas models (Wojcik-Pastuszka *et al*., 2019). The most suitable model for the release profile of nanoparticles was selected according to the determination coefficients (R^2).

In vitro transfection studies

Cells were seeded into 6-well plates at a density of 2 × 10^6 cells per well and incubated overnight. Transfections were performed on cells that were approximately 70% confluent. Before transfection, the medium was removed, and cells were rinsed with PBS (pH 7.4). Nanoparticle formulations and both free siRNAs (2µg of siRNA per well) in serum-free medium, were added to the cells. After the cells were incubated for 6 hours, the serum-containing medium was supplemented to the wells. After 48 hours, the culture medium was collected for VEGF ELISA assay.

In vitro cellular uptake studies

Cells (2×10^6) were seeded in a 6-well plate and incubated until 70% confluence. Then, transfection was performed with the nanoparticles containing fluorescein (FLO)-labelled siRNAs as mentioned before. Cellular uptake of nanoparticles was observed using a fluorescence microscope (Olympus CKX41, Japan) at different time intervals.

Determination of VEGF levels

VEGF protein that accumulated in the culture medium and recombinant human VEGF protein standards were analysed by sandwich ELISA. ELISA was performed for the cell culture medium according to the manufacturer's instructions (Invitrogen, CA, USA). Absorbances were measured spectrophotometrically at 450 nm. The percentage inhibition of VEGF expression was calculated in siRNA-transfected samples compared with untreated cells. Each test was repeated in triplicate, and standard deviations (SD) were calculated.

Apoptosis assay

The apoptosis study was performed with Caspase 3 colorimetric protease assays according to the manufacturer's protocol. Upon cleavage of the substrate by caspases, the absorbance of free pNA was measured by a microplate reader (Epoch, BioTek Instruments, USA) at 400 nm. Caspase activity was determined by comparing of the absorbance of apoptotic samples with an uninduced control.

Determination of IFN-γ levels

IFN-γ expression in cell culture medium was determined to observe whether siRNA-loaded nanoparticles induce IFN-γ *in vitro*, using ELISA assay according to the manufacturer's instructions. The absorbances of the standards and samples were measured spectrophotometrically at 450 nm. IFN-γ protein concentrations were determined according to the standard curve prepared from the standard dilutions. All measurements were performed in triplicate.

Statistical analyses

The results were expressed as the mean ± SD. The treatment groups were analysed using one-way ANOVA with Tukey's multiple comparisons test. All analyses were performed using GraphPad Prism 8.0.1 (GraphPad Software, San Diego, CA). $P<0.05$ was statistically significant.

RESULTS AND DISCUSSION

Characterisation of nanoparticles

The weight ratio of chitosan to TPP for the preparation of chitosan nanoparticles was selected to be 1:1 at which the best efficiency was observed. The results regarding the characterisation of nanoparticles are given in Table I. In our study, siRNA-loaded chitosan nanoparticles were positively charged and had a size between 268.2-311.8 nm. The success of tumour-targeting drug delivery systems is based on the nanoparticles' ability to accumulate in the desired tissues or cells. The enhanced permeability and retention (EPR) effect allows molecules of certain sizes (usually 100-1000 nm) to accumulate in tumour tissues rather than in normal tissues (Xin *et al*., 2017). It has been reported that 100-300 nm sized particles proposed for therapeutic use, can pass through the endothelial barriers given that the pore cut-off size in many tumours was between 380 and 780 nm (Hobbs *et al*., 1998).

We determined that the zeta potential values of all prepared nanoparticle formulations were positive (+) and close to neutral. Although a low-charge density contributes to low cytotoxicity and might facilitate the intracellular release of siRNA from the nanoparticles, this could also lead to particle aggregation and low stability (Malmo *et al.*, 2012).

TABLE I - Characterisation of chitosan nanoparticles

Preparations	Z-average (d.nm ± SD)	Zeta potential (mV± SD)	Encapsulation efficiency (% ± SD)
Blank CS NP	284.3 ± 9.2	14.5 ± 2.5	-
21-bp siRNA/CS NP	268.2 ± 47.3	9.0 ± 0.6	95.0 ± 3.9
35-bp siRNA/CS NP	311.8 ± 3.14	12.6 ± 1.3	89.0 ± 8.9

bp: Base pair, CS: Chitosan, d.nm: Diameter values in nanometres, mV: Millivolt, NP: Nanoparticle, SD: Standard deviation.

The morphology of the nanoparticles was observed with TEM. The images showed that some nanoparticles fell one by one, while others began to form aggregates (Figure 1). TEM results showed that the nanoparticles were irregularly shaped. Due to the shielding effect of NH groups of chitosan and the predominance of intramolecular hydrogen bonds during crosslinking, more chitosan molecules are involved in crosslinking, leading to the formation of larger particles and aggregates like flocculant structures (Fan *et al*., 2012).

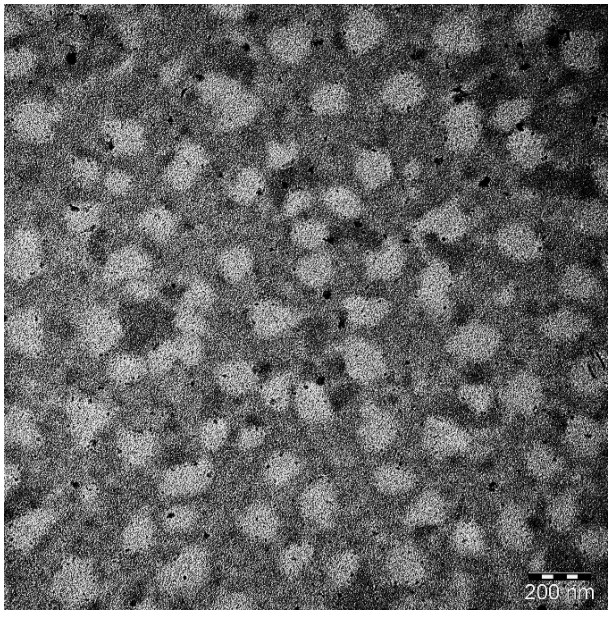

FIGURE 1 - Transmission electron microscopy images of chitosan nanoparticles at 75kx magnification.

Binding efficiency of siRNA to chitosan nanoparticles

21-bp and 35-bp siRNAs efficiently associated with chitosan nanoparticles were observed by agarose gel electrophoresis. Both siRNAs bound with chitosan were detained within the well (Figure 2). We also found that siRNAs were completely bound to chitosan nanoparticles due to the absence of a trailing band.

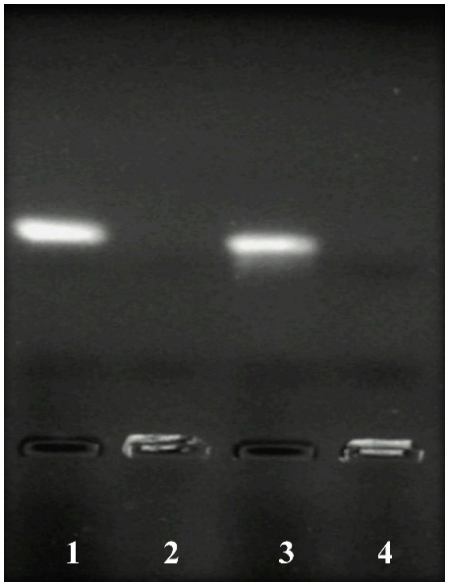

FIGURE 2 - Binding efficiency of siRNA-loaded chitosan nanoparticles. **1.** Free 21-bp siRNA, **2.** 21-bp siRNA/Chitosan Nanoparticle, **3.** Free 35-bp siRNA, **4.** 35-bp siRNA/Chitosan Nanoparticle.

Serum stability of siRNA-loaded nanoparticles

siRNA must be protected against nucleases to ensure high gene silencing efficiency in cells (Braasch *et al*., 2003). Therefore, the serum stability of chitosan/siRNA nanoparticles was examined in 10% FBS to determine whether the prepared formulations protect siRNAs from nuclease degradation (Figure 3). Degradation of the free siRNAs was observed after 1 hour. The 35-bp siRNA was fully degraded after 48 hours, but the complete degradation of 21-bp siRNA did not occur even after 48 hours (Figure 3A, 3B). The bands for chitosan/siRNA nanoparticles showed the migration of siRNA out from the nanoparticles after treatment with heparin (Figure 3C, 3D). siRNAs recovered from the nanoparticles appear to be protected from degradation for up to 48 hours. When free 21-bp and 35-bp siRNA were incubated with 10% FBS, changes in their structure occurred and degradation increased over time. Consequently, chitosan nanoparticles significantly protected both siRNAs from nuclease activity compared to free siRNAs.

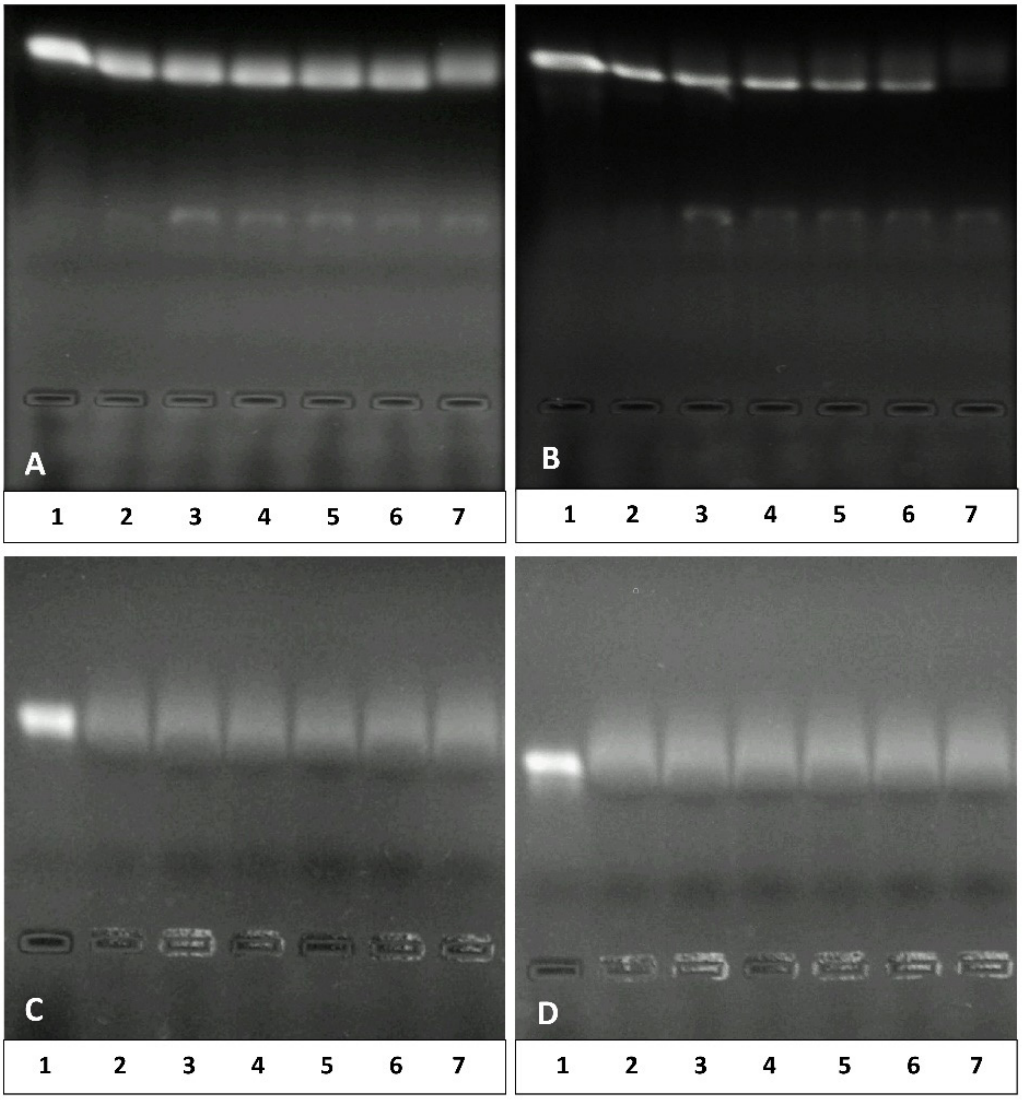

FIGURE 3 - Serum stabilities of free 21-bp siRNA (A), free 35-bp siRNA (B), 21-bp siRNA/Chitosan Nanoparticle (C) and 35-bp siRNA/Chitosan Nanoparticle (D) **1.** Free siRNA, **2-7.** 0, 1, 4, 6, 24, 48 hours. Serum stabilities of the nanoparticles and free siRNAs were determined in PBS (pH 7.4) with 10% FBS at 37°C. After heparin treatment of the nanoparticle samples, the integrity of the siRNAs was viewed on a 2% agarose gel.

Release properties of siRNA-loaded chitosan nanoparticles

The 21-bp and 35-bp siRNA released completely from chitosan nanoparticles in approximately 30 days (Figure 4). 21-bp siRNA and 35-bp siRNA were released from chitosan nanoparticles within the first 24 hours, resulting in 15% and 17% of cumulative release, respectively. Chitosan nanoparticles were found to have a burst effect in the release profile. The substance confined to the surface layer of the particle is dispersed immediately upon contact with the release medium and leads to a burst effect (Agnihotri, Mallikarjuna, Aminabhavi, 2004).

Comparison of the release profiles of chitosan nanoparticles with both 21-bp and 35-bp siRNAs revealed a similar release profile similar during 24 days. The release rate of siRNAs from the nanoparticles was rapid in the first step followed by a slower release due to the swelling of the polymer, with siRNAs continuously released at a constant rate but then released at an increased rate once again. It is thought that erosion and disintegration of nanoparticles might cause this rapid increase. Degradation of the polymer might cause subsequent physical erosion because of bond breaking, which shows that the degradation process correlates with the erosion of the polymer (Mohammed *et al*., 2017).

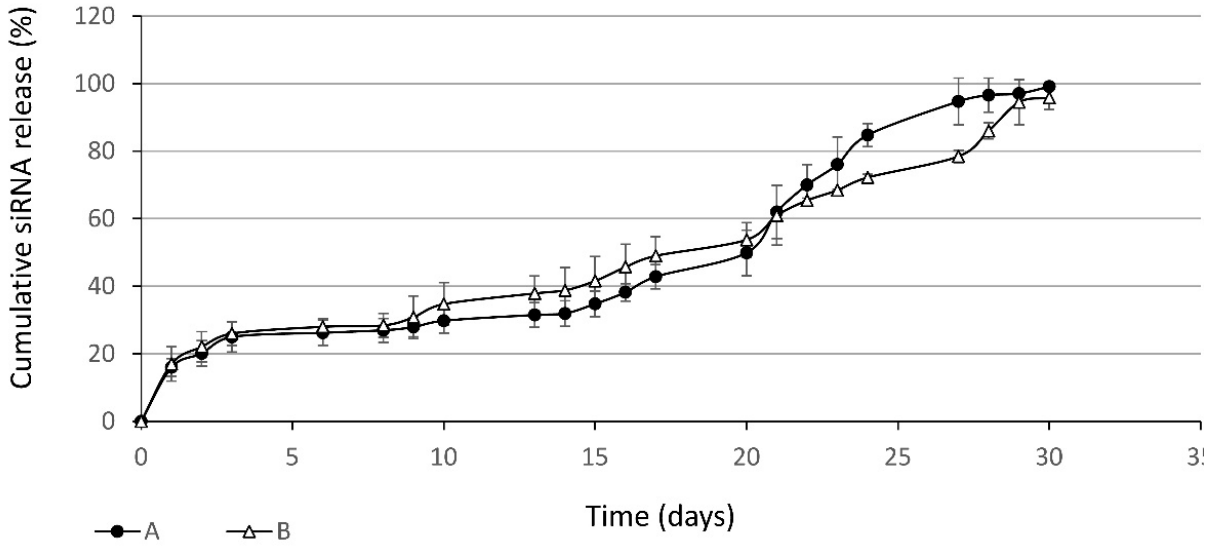

FIGURE 4 - The release profile of 21-bp siRNA/Chitosan Nanoparticle (A), and 35-bp siRNA/Chitosan Nanoparticle (B). The release study was performed in PBS (pH 7.4) at 37 °C.

According to the R^2 values, the zero-order kinetic model fits the release profile of both nanoparticles (Table II). In the zero-order kinetic model, the R^2 values for chitosan/ 21-bp siRNA and chitosan/ 35-bp siRNA nanoparticles were 0.9061 and 0.9578, respectively. Zero-order kinetics describes constant drug release from the drug delivery system independent of the concentration (Bhasarkar, Bal, 2019). The difference factor (f_1) and the similarity factor (f_2) calculated to compare the release profiles of both nanoparticles were found to be 10.28 and 59.64, respectively. The two release profiles are similar when the f_1 value is in the range of 0-15 and the f_2 value is in the range of 50-100 (Cano-Vega, Deng, Pinal, 2021).

TABLE II - The kinetic parameters of siRNA release from the chitosan nanoparticles

Kinetic Model	Chitosan/21-bp siRNA nanoparticle	Chitosan/35-bp siRNA nanoparticle
Zero-Order	R^2: 0.9061 k_0: 0.1209 (% x h^{-1})	R^2: 0.9578 k_0: 0.106 (% x h^{-1})
First-Order	R^2: 0.6754 k_1: 4.6 x 10^{-3} (h^{-1})	R^2: 0.7226 k_1: 2.9 x 10^{-3} (h^{-1})
Higuchi	R^2: 0.769 k_H: 3.326 (% x $h^{-1/2}$)	R^2: 0.8492 k_H: 2.9801 (% x $h^{-1/2}$)
Korsmeyer-Peppas	R^2: 0.7557 k_{KP}: 6,2806 (% x h^{-1}) n: 0.3485	R^2: 0.8218 k_{KP}: 7.4559 (% x h^{-1}) n: 0.3241
Hixson-Crowell	R^2: 0.7833 k_{HC}: 4.1 x 10^{-3} ($\%^{1/3}$ x h^{-1})	R^2: 0.8314 k_{HC}: 3.1 x 10^{-3} ($\%^{1/3}$ x h^{-1})

k_0: Zero-order release constant, k_1: First-order release constant, k_H: Higuchi release constant, k_{KP}: Korsmeyer-Peppas release constant, k_{HC}: Hixson-Crowell release constant, R^2: the coefficient of determination, n: the diffusional exponent, h: hour

Cellular uptake and intracellular distribution of nanoparticles

After transfecting the breast cancer cell lines with chitosan/5'-FLO siRNA nanoparticles, the cells were examined using fluorescence microscopy to establish the cellular uptake and distribution of siRNAs. Green fluorescence was intensely observed after transfection (Figure 5). Fluorescence from chitosan/5'-FLO siRNA nanoparticles was mostly distributed in the cytoplasm similar to previous observations (Raja, Katas, Wen, 2015).

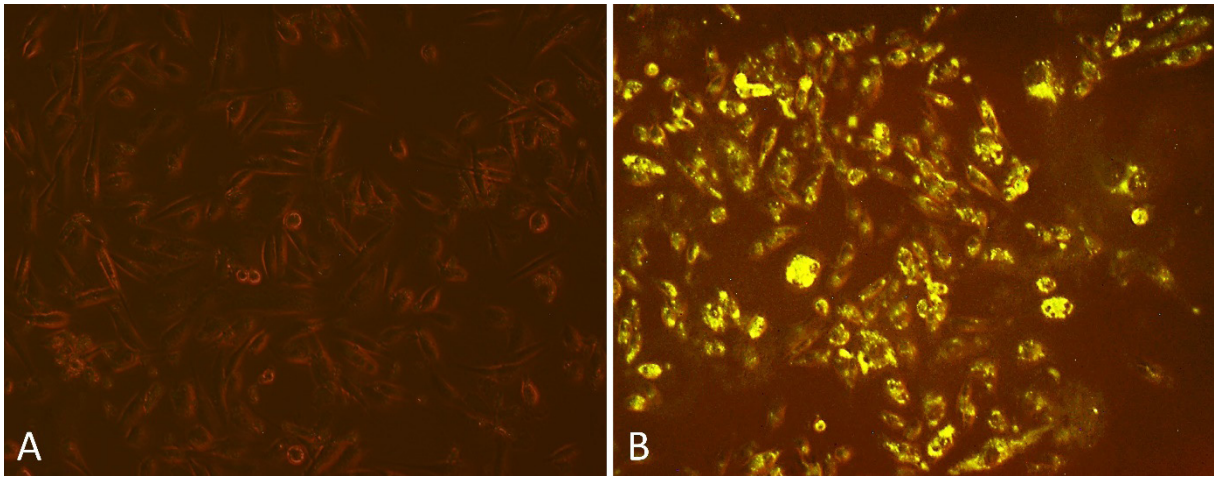

FIGURE 5 - Fluorescence microscopy images of cellular uptake after transfection with chitosan nanoparticles in MDA-MB-231 cells (10 x magnification). (A) Blank chitosan nanoparticles, (B) Chitosan /5'-FLO siRNA nanoparticles (fluorescein-labelled).

Effects of nanoparticles on VEGF expression

After MDA-MB-231 cells were transfected with chitosan/21-bp and chitosan/35-bp siRNA nanoparticles, VEGF levels in cells were determined using ELISA. As seen in Figure 6, both chitosan/21-bp and chitosan/35-bp siRNA nanoparticles provided significant gene silencing compared to the control group ($p<0.01$). Chitosan/21-bp siRNA and chitosan/35-bp siRNA nanoparticles reduced VEGF levels by 69.6% and 51.2%, respectively. These results show that chitosan-TPP nanoparticles are a suitable gene delivery system for introducing siRNA into cells, as stated in previous studies (Katas, Alpar, 2006; Raja, Katas, Wen, 2015; Rojanarata *et al*., 2008). We found that chitosan/21-bp siRNA nanoparticles had statistically higher gene silencing activity than chitosan/35-bp siRNA nanoparticles ($p<0.01$). Similarly, Kim *et al*. (2005) reported that RNAi activity of dsRNAs longer than 27 nt gradually decreased.

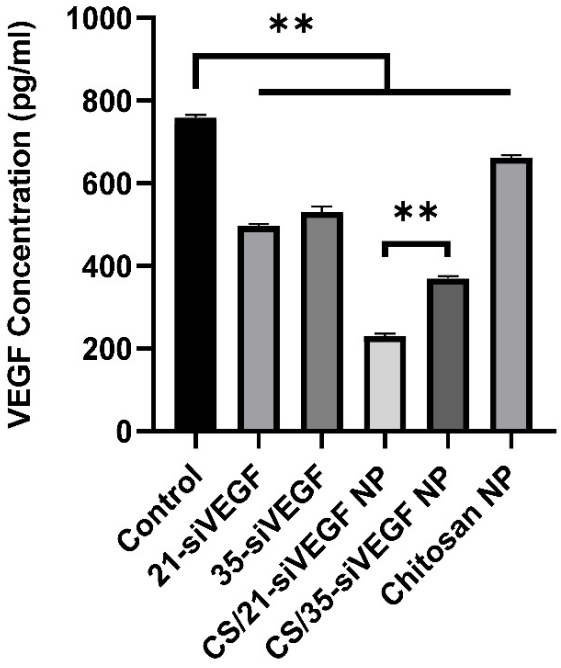

FIGURE 6 - VEGF levels after transfection with siRNA-loaded chitosan nanoparticles in MDA-MB-231 cells. VEGF concentrations were determined by ELISA assay. 2µg of siRNA was applied to each group, excluding the control group. Results were shown as mean ± SD (n =3). VEGF silencing efficiency was estimated according to the control group (no treatment). ** indicates $p<0.01$. 21-siVEGF: 21-bp siRNA targeting VEGF gene, 35-siVEGF: 35-bp siRNA targeting VEGF gene, CS: Chitosan, NP: Nanoparticle.

Effects of nanoparticles on apoptosis

Dysregulated cell proliferation and suppression of apoptosis cause tumorigenesis and tumour growth. Anticancer therapeutics are thought to cause the death of tumour cells by inducing apoptosis (Peng *et al*., 2013). Ge *et al*. (2009) reported that the inhibition of VEGF with siRNA increased apoptosis in MCF-7 breast cancer cell lines. The caspase protease activity assay was used to analyse apoptosis (Figure 7). Chitosan/21-bp and chitosan/35-bp siRNA nanoparticles increased caspase activity by 2-fold and 1.75-fold compared with the control group, respectively. Both siRNA-loaded chitosan nanoparticles significantly increased caspase activity compared to the control group in MDA-MB-231 cells. The difference between chitosan/21-bp and chitosan/35-bp siRNA nanoparticles for the increase in caspase activity was not statistically significant ($p= 0.4652$).

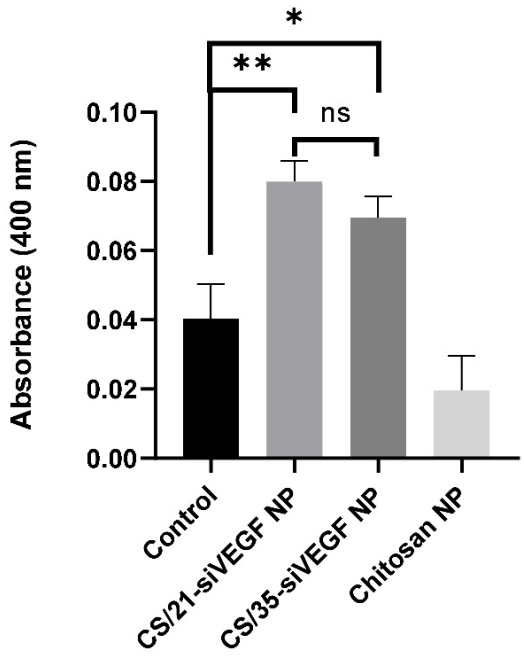

FIGURE 7 - Caspase protease activity after transfection with siRNA-loaded chitosan nanoparticles in MDA-MB-231 cells. Apoptosis was induced by incubating the cells with the chitosan nanoparticles for 48 hours. 2µg of siRNA was applied to each group, excluding the control group. * indicates $p<0.05$ and ** indicates $p<0.01$ compared with the control group (no treatment). Results were shown as mean ± SD (n =3). 21-siVEGF: 21-bp siRNA targeting VEGF gene, 35-siVEGF: 35-bp siRNA targeting VEGF gene, CS: Chitosan, NP: Nanoparticle, ns: non-sense.

Effects of nanoparticles on IFN-γ expression

siRNAs lead to activate the mammalian innate immune system. Synthetic siRNAs can promote high level expression of inflammatory cytokines and interferons (Judge, MacLachlan, 2008). Interferons are cytokines that are responsible for activating the immune system and have antiviral and antitumor effects (Castro *et al*, 2018). Also, treatment of IFN-γ has been shown to suppress the growth of breast and ovarian cancer cells, both *in vitro* and *in vivo* and induce apoptosis (Treeck *et al*., 2005). Production of IFN-γ is mostly seen in T lymphocytes and NK cells. The expression of IFN-γ mRNA in other cell types is very low (Castro *et al*, 2018). However, Xue, Firestone, and Bjeldanes (2005) were the first group to report that IFN-γ gene transcription could be induced in human breast cancer cell lines such as MCF-7 and MDA-MB-231. We examined whether chitosan/21-bp and chitosan/35-bp siRNA nanoparticles induce IFN-γ expression in MDA-MB-231. After transfection, IFN-γ levels were determined by ELISA. IFN-γ expression was not observed in the control groups, but only induced in the cells treated with chitosan nanoparticles (Figure 8). As the free 21-bp and 35-bp siRNA did not generate IFN-γ responses, they are not shown in Figure 8. siRNAs induced cytokine activation in a dose-dependent and sequence-independent manner by applying siRNAs with transfection agents, not only siRNA (Lee *et al*., 2012). All chitosan nanoparticles caused a significant increase in IFN-γ protein levels compared to the control group ($p<0.01$). The blank chitosan nanoparticles also induced IFN-γ expressions *in vitro*, suggesting that this effect is related to chitosan. Chitosan and its derivatives are widely investigated as adjuvant and vaccine delivery systems due to their immunostimulatory effects (Vasiliev, 2014). It was reported that chitosan induced expression of IFN-γ at low levels in lung epithelial cells when administered alone and intranasally to mice (Kumar *et al*., 2003). Chitosan/35-bp siRNA nanoparticles induced IFN-γ at a greater level than chitosan/21-bp siRNA nanoparticles ($p<0.01$).

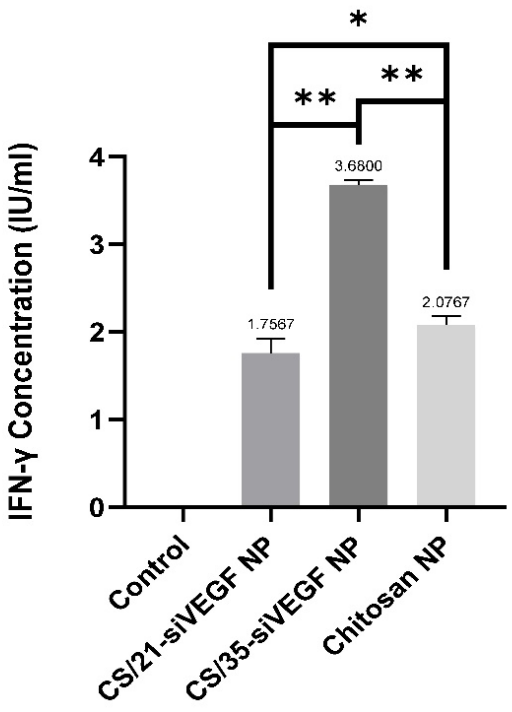

FIGURE 8 - Effect of the nanoparticles on IFN-γ expression in MDA-MB-231 cells. Human IFN-γ concentration in the cell culture medium was determined by ELISA 48 hours after transfection. 2μg of siRNA was applied to each group, excluding the control group. Results were shown as mean ± SD (n =3). * indicates $p<0.05$ and ** indicates $p<0.01$. 21-siVEGF: 21-bp siRNA targeting VEGF gene, 35-siVEGF: 35-bp siRNA targeting VEGF gene, CS: Chitosan, NP: Nanoparticle.

CONCLUSION

In summary, we demonstrated that chitosan nanoparticles prepared with long siRNAs consisting of 35 bp inhibited VEGF gene expression and induced apoptosis in MDA-MB-231 cells which was also seen with 21-bp siRNAs. We also observed that the characteristics and release profiles of chitosan nanoparticles prepared with both siRNAs were similar. The release kinetics of siRNAs from chitosan nanoparticles were found to best fit the zero-order kinetic model for both nanoparticles. Moreover, we observed that chitosan nanoparticles stimulated IFN-γ expression *in vitro*, when used as a delivery system. This feature of chitosan nanoparticles is thought to positively contribute to siRNA-related anticancer effect through VEGF gene inhibition.

ACKNOWLEDGMENTS

This study was supported by the Marmara University Scientific Research Projects Association (SAG-C-YLP-071015-0466).

DECLARATION OF CONFLICTING INTERESTS

The authors declare no conflict of interest.

REFERENCES

Agnihotri SA, Mallikarjuna NN, Aminabhavi TM. Recent advances on chitosan-based micro-and nanoparticles in drug delivery. J Control Release. 2004; 100(1): 5-28.

Amarzguioui M, Lundberg P, Cantin E, Hagstrom J, Behlke MA, Rossi JJ. Rational design and in vitro and in vivo delivery of Dicer substrate siRNA. Nat Protoc. 2006; 1(2):508-517.

Ayoub NM, Jaradat SK, Al-Shami KM, Alkhalifa AE. Targeting Angiogenesis in Breast Cancer: Current Evidence and Future Perspectives of Novel Anti-Angiogenic Approaches. Front Pharmacol. 2022; 3:838133.

Bhasarkar J, Bal D. Kinetic investigation of a controlled drug delivery system based on alginate scaffold with embedded voids. J Appl Biomater Funct Mater. 2019;17(2).

Braasch DA, Jensen S, Liu Y, Kaur K, Arar K, White MA, et al. RNA interference in mammalian cells by chemically-modified RNA. Biochemistry. 2003;42(26):7967-7975.

Calvo P, Remunan-Lopez C, Vila-Jato JL, Alonso MJ. Chitosan and chitosan/ethylene oxide-propylene oxide block copolymer nanoparticles as novel carriers for proteins and vaccines. Pharm Res. 1997;14(10):1431-1436.

Cano-Vega MA, Deng M, Pinal R. Modular solid dosage form design – Application to pH-independent release of a weak-base API. Int J Pharm. 2021;601:120518.

Castro F, Cardoso AP, Gonçalves RM, Serre K, Oliveira MJ. Interferon-Gamma at the Crossroads of Tumor Immune Surveillance or Evasion. Front Immunol. 2018;9:847.

Chang CI, Kang HS, Ban C, Kim S, Lee DK. Dual-target gene silencing by using long, synthetic siRNA duplexes without triggering antiviral responses. Mol Cells. 2009;27(6):689-695.

Chen J, Sun X, Shao R, Xu Y, Gao J, Liang W. VEGF siRNA delivered by polycation liposome-encapsulated calcium phosphate nanoparticles for tumor angiogenesis inhibition in breast cancer. Int J Nanomed. 2017;12:6075-6088.

Dahlgren C, Wahlestedt C, Thonberg H. No induction of anti-viral responses in human cell lines HeLa and MCF-7 when transfecting with siRNA or siLNA. Biochem Biophys Res Commun. 2006;341(4):1211-1217.

Dong D, Gao W, Liu Y, Qi XR. Therapeutic potential of targeted multifunctional nanocomplex co-delivery of siRNA and low-dose doxorubicin in breast cancer. Cancer Lett. 2015;359(2):178-186.

Elbashir SM, Harborth J, Lendeckel W, Yalcin A, Weber K, Tuschl T. Duplexes of 21-nucleotide RNAs mediate RNA interference in cultured mammalian cells. Nature. 2001;411(6836):494-498.

Fan W, Yan W, Xu Z, Ni H. Formation mechanism of monodisperse, low molecular weight chitosan nanoparticles by ionic gelation technique. Colloids Surf B Biointerfaces. 2012;90:21-27.

Feng Q, Yu MZ, Wang JC, Hou WJ, Gao LY, Ma XF, et al. Synergistic inhibition of breast cancer by co-delivery of VEGF siRNA and paclitaxel via vapreotide-modified core-shell nanoparticles. Biomaterials. 2014;35(18):5028-5038.

Ge YL, Zhang X, Zhang JY, Hou L, Tian RH. The mechanisms on apoptosis by inhibiting VEGF expression in human breast cancer cells. Int Immunopharmacol. 2009;9(4):389-395.

Hobbs SK, Monsky WL, Yuan F, Roberts WG, Griffith L, Torchilin VP, et al. Regulation of transport pathways in tumor vessels: role of tumor type and microenvironment. Proc Natl Acad Sci U S A. 1998;95(8):4607-4612.

Holliday DL, Speirs V. Choosing the right cell line for breast cancer research. Breast Cancer Res. 2011;13(4):215.

Judge A, MacLachlan I. Overcoming the Innate Immune Response to Small Interfering RNA. Hum Gene Ther. 2008;19(2):111-124.

Katas H, Alpar HO. Development and characterisation of chitosan nanoparticles for siRNA delivery. J Control Release. 2006;115(2):216-225.

Kim DH, Behlke MA, Rose SD, Chang MS, Choi S, Rossi JJ. Synthetic dsRNA Dicer substrates enhance RNAi potency and efficacy. Nat Biotechnol. 2005;23(2):222-226.

Kim DH, Rossi JJ. RNAi mechanisms and applications. Biotechniques. 2008;44(5):613–616.

Kumar M, Kong X, Behera AK, Hellermann GR, Lockey RF, Mohapatra SS. Chitosan IFN-γ-pDNA Nanoparticle (CIN) Therapy for Allergic Asthma. Genet Vaccines Ther. 2003;1(1):3.

This is an open-access article distributed under the terms of the Creative Commons Attribution License.

Lee HW, Choi SJ, Yoo YM, Sohn JH, Koh SB, Park KS. Apoptosis induced by nonspecific effects of siRNA in human umbilical vein endothelial cell. Toxicol Environ Health Sci. 2012;4(1):50-56.

Leung AKK, Tam YYC, Cullis PR. Lipid nanoparticles for short interfering RNA delivery. Adv Genet. 2014;88:71–110.

Malmo J, Sørgård H, Vårum KM, Strand SP. siRNA delivery with chitosan nanoparticles: Molecular properties favoring efficient gene silencing. J Control Release. 2012;158(2):261-268.

Mohammed MA, Syeda JTM, Wasan KM, Wasan EK. An Overview of Chitosan Nanoparticles and Its Application in Non-Parenteral Drug Delivery. Pharmaceutics. 2017;9(4):53.

Ozcan G, Ozpolat B, Coleman RL, Sood AK, Lopez-Berestein G. Preclinical and clinical development of siRNA-based therapeutics. Adv Drug Deliv Rev. 2015;87:108-119.

Peng W, Chen J, Qin Y, Yang Z, Zhu YY. Long double-stranded multiplex siRNAs for dual genes silencing. Nucleic Acid Ther. 2013;23(4):281-288.

Raja MA, Katas H, Jing Wen T. Stability, Intracellular Delivery, and Release of siRNA from Chitosan Nanoparticles Using Different Cross-Linkers. PLoS One. 2015;10(6):e0128963.

Rojanarata T, Opanasopit P, Techaarpornkul S, Ngawhirunpat T, Ruktanonchai U. Chitosan-thiamine pyrophosphate as a novel carrier for siRNA delivery. Pharm Res. 2008;25(12):2807-2814.

Rudzinski WE, Aminabhavi TM. Chitosan as a carrier for targeted delivery of small interfering RNA. Int J Pharm. 2010;399(1-2):1-11.

Treeck O, Kindzorra I, Pauser K, Treeck L, Ortmann O. Expression of icb-1 gene is interferon-gamma inducible in breast and ovarian cancer cell lines and affects the IFN gamma-response of SK-OV-3 ovarian cancer cells. Cytokine. 2005;32(3-4):137-142.

Vasiliev YM. Chitosan-based vaccine adjuvants: incomplete characterization complicates preclinical and clinical evaluation. Expert Rev Vaccines. 2014;14(1):37-53.

Wojcik-Pastuszka D, Krzak J, Macikowski B, Berkowski R, Osiński B, Musiał W. Evaluation of the Release Kinetics of a Pharmacologically Active Substance from Model Intra-Articular Implants Replacing the Cruciate Ligaments of the Knee. Materials (Basel). 2019;12(8):1202.

Xin Y, Yin M, Zhao L, Meng F, Luo L. Recent progress on nanoparticle-based drug delivery systems for cancer therapy. Cancer Biol Med. 2017;14(3):228-241.

Xue L, Firestone GL, Bjeldanes LF. DIM stimulates IFN gamma gene expression in human breast cancer cells via the specific activation of JNK and p38 pathways. Oncogene. 2005;24(14):2343-2353.

Zarychta E, Ruszkowska-Ciastek B. Cooperation between Angiogenesis, Vasculogenesis, Chemotaxis, and Coagulation in Breast Cancer Metastases Development: Pathophysiological Point of View. Biomedicines. 2022;10:300.

Received for publication on 09th June 2022
Accepted for publication on 07th December 2022